Clinical Case Report

Medicine®

OPEN

The role of 18F-FDG PET/CT in management of paraneoplastic limbic encephalitis combined with small cell lung cancer

A case report

Helga Castagnoli, MD[a,*], Carlo Manni, MD[a], Francesca Marchesani, MD[b], Gloria Rossi, MP[c], Sara Fattori, MP[c], Francesca Capoccetti, MD[a]

Abstract

Rationale: Limbic encephalitis is one of the most common paraneoplastic neurological disorders (PND). The role of brain Fluorine-18-fluorodeoxyglucose position emission tomography/computed tomography (CT) in paraneoplastic limbic encephalitis (PLE) and of the whole body 18F-FDG PET/CT in this setting, remains still not well defined.

Patient concerns: We report a case of a patient with chronic inflammatory rheumatism, psoriasis and Hashimoto thyroiditis and subsequent appearance of static and dynamic ataxia and episodic memory deficit who was diagnosed as PLE combined with small cell lung cancer (SCLC).

Diagnoses: The diagnosis of SCLC was made with EBUS-TBNA of a mediastinal lymph node.

Interventions: Whole-body 18F-FDG PET/CT was performed for the initial staging of SCLC, in the planning of radiotherapy treatment, to evaluate therapeutic response and in the follow-up. A dedicated brain scan was included to the same PET session. Whole-body contrast enhanced computed tomography (CT) and contrast enhanced whole-brain MRI were also performed.

Outcomes: She was administered neoadjuvant chemioterapy with Cisplatin and Etoposide with concomitant radiotherapy treatment. Whole body 18F-FDG PET/CT showed a complete metabolic response already after 3 cycles of chemioterapy. Brain functional study showed a metabolic pattern characterized by the migration of hypermetabolism in the bilateral hippocampal areas during the therapeutic treatment, which correlated with the persistence of clinical symptoms.

Lessons: In the era of personalized medicine and targeted therapy, this case highlights the importance of the 18F-FDG PET/CT study as an accurate tool to identify PLE and to guide the diagnostic work-up of the underlying tumor. Considering that most of these are 18F-FDG avid tumors and that the 18F-FDG PET/CT scan is often added to the diagnostic work-up when screening patients for malignancy, this functional imaging can play a decisive role.

Abbreviations: 18F-FDG PET/CT = fluorine-18-fluorodeoxyglucose position emission tomography/computed tomography, AbTPO = thyroperoxidase antibodies was elevated, AE = autoimmune encephalitis, AFP = alpha-fetoprotein, ANA = Anti-nuclear Antibody, ANCA = anti-neutrophil cytoplasmic antibodies, ATA = American Thyroid Association, Ca 125 = cancer antigen 125, Ca 15-3 = cancer antigen 15-3, Ca 19-9 = cancer antigen 19-9, CASPR2 = contactin-associated protein-like 2, CEA = carcinoembryonic antigen, CRP = C-reactive protein, CSF = cerebrospinal fluid, CT = computed tomography, DWI = diffusion weighted imaging, EBUS-TBNA = endobronchial ultrasound-guided transbronchial needle aspiration, EEG = electroencephalography, EFS = event-free survival, ENA SS-A = Extractable Nuclear Antigen, ENT = ear, nose and throat, EORTC = European Organization for Research and Treatment of Cancer, FLAIR = fluid attenuated inversion recovery, FNA = fine needle aspiration, GABA B = Gamma-Aminobutyric acid-B, GAD = glutamic acid decarboxylase, GLUR3 = glutamate receptor subtype 3, HIV = human immunodeficiency virus, IGEV = Ifosfamide, Gemcitabine, Vinorelbine, LE = limbic encephalitis, LGI1 = leucine-rich glioma-inactivated 1, MRI = magnetic resonance imaging, NCCN = National Comprehensive Cancer Network, NMDAR = anti-N-methyl-D-aspartate receptor, NSE = neuron specific enolase, OS = overall survival, PERCIST = Positron Emission Tomography Response Criteria In Solid Tumors, PLE = paraneoplastic limbic encephalitis, PND = paraneoplastic neurological disorders, PNMA2 = paraneoplastic antigen Ma2, SCLC = small cell lung cancer, SUV Max = Maximum Standardized Uptake Value, TNM = Tumor-

Editor: N/A.

Informed written consent was obtained from the patient for publication of this case report and accompanying images.

The authors have no conflicts of interests to disclose.

[a] Service Department Macerata Hospital, ASUR Marche AV3, Nuclear Medicine Unit, [b] Pulmonary Unit ASUR Marche AV3, [c] Service Department Macerata Hospital, ASUR Marche AV3, Medical Physics Unit, Macerata, Italy.

[*] Correspondence: Helga Castagnoli, Ospedale di Macerata, Macerata, Italy (e-mail: helgacastagnoli@gmail.com).

Medicine (2019) 98:35(e16593)

Received: 9 January 2019 / Received in final form: 22 May 2019 / Accepted: 2 July 2019

http://dx.doi.org/10.1097/MD.0000000000016593

Nodes-Metastasis, TPA = tissue polypeptide antigen, TPHA = Treponema pallidum Hemagglutination Assay, TSH = thyroid stimulating hormone, VGKC = voltage-gated potassium channel.

Keywords: Brain 18F-FDG PET/CT, paraneoplastic limbic encephalitis, paraneoplastic neurological disorders, small cell lung cancer, whole-body 18-FDG PET/CT

1. Introduction

Paraneoplastic neurological disorders (PND) usually develop before an underlying tumor is recognized, often leading to tumor diagnosis.[1] Early recognition of PND is helpful for the tumor treatment. In 60% of patients with PND the neurologic symptoms develop before cancer is diagnosed that why these patients are usually seen first by general practitioners or neurologists.[2] Limbic encephalitis is one of the most common PND. It is an inflammatory process highly confined to structures of the limbic system.

There are several disorders unrelated to cancer that may cause limbic dysfunction such as autoimmune systemic disorders (Lupus erythematosus, Hashimoto encephalitis, Sjögren syndrome), infection, toxic metabolic encephalopathy, primary angiitis of the central nervous system, brain tumors and syphilis.

The tumors more frequently associated with limbic encephalitis are small cell lung cancer (SCLC), testicular tumors, teratoma of the ovary, Hodgkin lymphoma and breast cancer.[3]

A paraneoplastic etiology can only be established with the demonstration of paraneoplastic antibodies in the serum or cerebrospinal fluid (CSF) or with the demonstration of a tumor.[4]

A potential role of the Brain fluorodeoxyglucose-PET/CT in the evaluation of the autoimmune encephalitis and in particular in paraneoplastic limbic encephalitis (PLE) has been previously described.[2,5,6] According to the authors, metabolic neuroimaging is especially useful in patients without seizures and normal magnetic resonance imaging (MRI).[7] Moreover, Brain 18F-FDG PET/CT findings have been more clearly associated with the clinical picture, disease severity, and recovery after therapy than MRI findings.[8] At the moment, in most patients with PND, whole body 18F-FDG PET/CT scan should be reserved when conventional imaging (CT scan) fails to identify a tumor or when lesions are difficult to biopsy.[9]

In this report, we present the case of a patient with Hashimoto thyroiditis and subsequent appearance of static and dynamic ataxia who was diagnosed as PLE combined with SCLC. We analyzed PLE metabolic characteristic of this patient before and after immunotherapy and we evaluated the utility of the whole body 18F-FDG PET/CT in the detection of malignancy, tumor staging, planning of the initial treatment, and monitored response to the therapy.

2. Case presentation

A 55 year-old woman presented with a 2-months history of pain in the joints, in particular the hips and the small joints of the hands associated with sensation of falling asleep of the feet first and then of the hands, prevalently to the left hand. For this symptomatology the patient had already performed rheumatological examination and anti-inflammatory therapy. The patient was a current smoker (10–15 cigarettes per day) and had chronic inflammatory rheumatism and psoriasis.

Subsequently a movement disorder appeared with postural instability and progressive improvement and she was admitted in our Hospital and examined by Neurologists, on February 23, 2017.

On admission, she was an alert, oriented and collaborating patient. The blood pressure was 110/70 mm Hg, the pulse rate was 70 per minute with regular body temperature and normal blood glucose. Neurological examination revealed cranial nerves in the norm, static and dynamic ataxia, slight dysmetria at the finger-to-nose test and mild hypo pallesthesia in the lower limbs. There was an autonomous walking with an enlarged base for short stretches. Ear, nose, and throat (ENT) examination excluded a peripheral vestibular pathology. A CT scan of the brain excluded the presence of intracranial hemorrhages. The routine blood was normal except for the platelet count 366,000/mmc, total protein 6.4 g/dl and serum sodium 134 meq/L. Serum protein electrophoresis, ferritin, β2 microglobulin, folic acid, and vitamin B12 showed no abnormality. Also C-reactive protein (CRP) and erythrocyte sedimentation rate were in the norm. The tests for hepatitis B and C, TPHA (Treponema pallidum Hemagglutination Assay) and human immunodeficiency virus (HIV) were negative. Thyroid stimulating hormone (TSH) and Thyroglobulin antibodies were within normal limits while Thyroperoxidase antibodies was elevated (AbTPO 115.5 UI/ml). In fact the patient had previously come to our Nuclear Medicine Department in 2008 for periodic checkups related to the diagnosis of Hashimoto thyroiditis. She was in therapy with levothyroxine. On rheumatology tests, C3, C4, and anti-neutrophil cytoplasmic antibodies (ANCA) were negative meanwhile Anti-nuclear Antibody (ANA) was positive (1:160, granular) and Extractable Nuclear Antigen (ENA SS-A) was positive (74.0 U/ml). The serum immunoglobulin test showed normal IgM e IgA and IgG below normal limits (801 mg/dl).

Oncological markers such as carcinoembryonic antigen (CEA), cancer antigen 19–9 (Ca 19–9), cancer antigen 125 (Ca 125), cancer antigen 15–3 (Ca 15–3), tissue polypeptide antigen (TPA), and alpha-fetoprotein (AFP) were within normal limits apart from neuron specific enolase (NSE) that was positive 23 microg/L (<15.2).

A contrast enhanced whole-brain MRI with including diffusion sequences was done and revealed a swollen left hippocampus with hyperintense signals on FLAIR (fluid attenuated inversion recovery) and on T2-weighted images. On T1 images the left hippocampus was hypointense for the edema's presence. The same signal alteration was also present in the right hippocampal and parahippocampal areas, but with less evidence. Signs of widespread restriction in DWI (diffusion weighted imaging) were also evident in the cortex of temporal lobes with contrast by the temporal horn of the lateral left ventricle. A diagnosis of possible acute limbic encephalitis (LE) with suspected ependymite of the temporal horn of the left lateral ventricle was carried out.

The patient underwent lumbar puncture and CSF analysis was performed; 11 cells/mmc were detected, protein was 1.28 g/L, glucose and chloride levels were normal. It was negative for viral infections and cytological abnormalities, but it revealed numerous oligoclonal bands, intrathecal IgG synthesis, and blood–brain barrier damage.

The onconeural antibodies against Yo, Ri, amphiphysin, and CV21 were all negative, but anti-PNMA2 (+) and anti-Hu (++++) were positive. CSF and peripheral blood were also tested for antibodies against neuronal cell surface antigens such as NMDAR, CASPR2, GABA B, VGKC, LGI1, and no antibody was detected. Also antibodies against the intracellular antigen glutamic acid decarboxylase (GAD) were negative. On the contrast antibodies to glutamate receptor subtype 3 (GluR3 A and B) were positive in the cerebrospinal fluid and normal in the blood.

After admission, the patient received high dose steroids (methylprednisolone 1 g/d i.v. for 5 days) for the treatment of encephalitis, followed by maintenance with oral prednisone (25 mg/d).

A contrast enhanced CT-scan of chest and abdomen was performed for the detection of unknown primary tumor. It showed a nodule with irregular margins at the apex of the right lung, a lymphadenopathy mass in Barety space and other lymph nodes at the level of the epiaortic vessels and at the right hilum.

A pulmonary neoplasm was then suspected to be contributing to the LE, and Endobronchial ultrasound-guided transbronchial needle aspiration (EBUS-TBNA) of lymph node (Station 4R) was performed. Waiting for the result, the patient was referred to our Nuclear Medicine Department for a staging 18F-FDG PET/CT scan (Fig. 1A–F). The study showed a focal hypermetabolic area at the apex of the right lung as well as voluminous, intensely-increased activity mass in Barety space. There was no significant uptake on the other mediastinal and right hilar lymph nodes showed on the CT-scan. In addition, there was focal thyroid uptake to the left lobe. The examination was extended at the brain level. Functional brain imaging detected significant asymmetric hypermetabolism of the bilateral mesial temporal lobe, with diffuse and intensely hypermetabolism in the left hippocampus and parahippocampal gyrus. However, even the right hippocampal activity was slightly increased compared to the normal one, especially in its antero-superior portion. Normal metabolism was detected in other cortical and subcortical structures and in the cerebellum.

A few days after the 18F-FDG PET/CT study, the patient underwent in our department, a fine needle aspiration (FNA) of a thyroid nodule. The cytological response was suggestive for the diagnosis of nodular hyperplasia.

On March 8, pathologic anatomy revealed that the lymph node (Station 4R) had the involvement of small cell neuroendocrine lung carcinoma. According to the 18F-FDG PET/CT result that showed no distant metastasis, the TNM Staging was cT1a cN2 Mx (Stage IIIA, *AJCC 7th Edition*).

On March 15, the patient started neoadjuvant chemioterapy with Cisplatin and Etoposide with concomitant radiotherapy treatment (total dose of 60 Gy) at the pulmonary and mediastinal levels.

On April 7, the patient was re-evaluated by the neurology colleagues. There was a progressive accentuation of the difficulty in keeping upright and walking. On the neurological objective examination the patient appeared vigilant, collaborating, and partially oriented in time and space with short-term episodic memory deficit. Moreover static and dynamic ataxia prevalent in the lower limbs was confirmed. The patient received immunomodulatory therapy with Ifosfamide, Gemcitabine, and Vinorelbine (IGEV) for 3 cycles and continued therapy with oral prednisone.

In May 2017, after 3 cycles of chemioterapy, an oncologic restaging with contrast enhanced CT and 18F-FDG PET/CT and was made. A full-body CT scan showed persistent of the pulmonary neoplastic disease (reduction of the maximum diameter of 12 mm vs 15 mm) and significant size reduction of mediastinal lymph nodes. Brain CT showed neither focal lesions nor encephalo-meningeal pathological contrast reinforcements. On 18F-FDG-PET/CT, the intense uptake in the right lung disappeared with associated significant metabolic reduction in Barety space.

Functional brain imaging detected widespread and homogeneous uptake in the right hippocampal and parahippocampal areas, while the left hippocampal hypermetabolism was significantly reduced (Fig. 2A–D)

During the steroid treatment, the patient reported a clinical benefit with improvement of some neurological symptoms. However, the inability to stand upright and also an incomplete movement in the left upper limb persisted.

Few months after the end of the chemo-radiotherapeutic treatment the patient underwent 18F-FDG-PET/CT scan. The study confirmed the absence of significant metabolism in the Barety lodge and at the right lung apex. The 18F-FDG PET/CT brain imaging showed hypermetabolism in the right hippocampal and para-hippocampal area, but less intense compared to the previous PET/CT.

Moreover the reappearance of intense uptake in the left hippocampus was observed as in the staging PET/CT (Fig. 3A–B).

After brain PET/CT findings, a reassessment of the framework with whole-brain MRI was requested. It showed hyperintense signals in both hippocampal areas, with prevalence of the left side on fluid attenuated inversion recovery (FLAIR) and T2-weighted images.

On January 10, 2018 a follow-up with 18F-FDG PET/CT was carried-out. The PET study confirmed the good metabolic response in the lung and lymph node. The appearance of a small focal hypermetabolic area near the right tonsil was highlighted, for which an ENT visit was recommended. It showed a slight hypertrophy of the lower pole of the right tonsil. Imaging of brain glucose metabolism revealed symmetrically decreased 18F-FDG uptake in the medial temporal lobes, although still slightly higher than the para-physiological uptake (Fig. 4A–E).

The patient has provided informed consent for publication of the case.

3. Discussion

Recently, Graus, and colleagues published in Lancet Neurology,[10] proposing a new syndrome-based diagnostic approach to the autoimmune encephalitis (AE); the criteria for the diagnosis of autoimmune limbic encephalitis were also revised.

For this diagnosis, 4 criteria need to be fulfilled:

1. Subacute onset (rapid progression of less than 3 months) of working memory deficits, seizures, or psychiatric symptoms suggesting involvement of the limbic system;
2. Bilateral brain abnormalities on T2-weighted fluid-attenuated inversion recovery MRI highly restricted to the medial temporal lobes;
3. At least 1 of the following:
   - CSF pleocytosis (white blood cell count of more than 5 cells per mm^3),
   - EEG with epileptic or slow-wave activity involving the temporal lobes;
4. Reasonable exclusion of alternative causes.

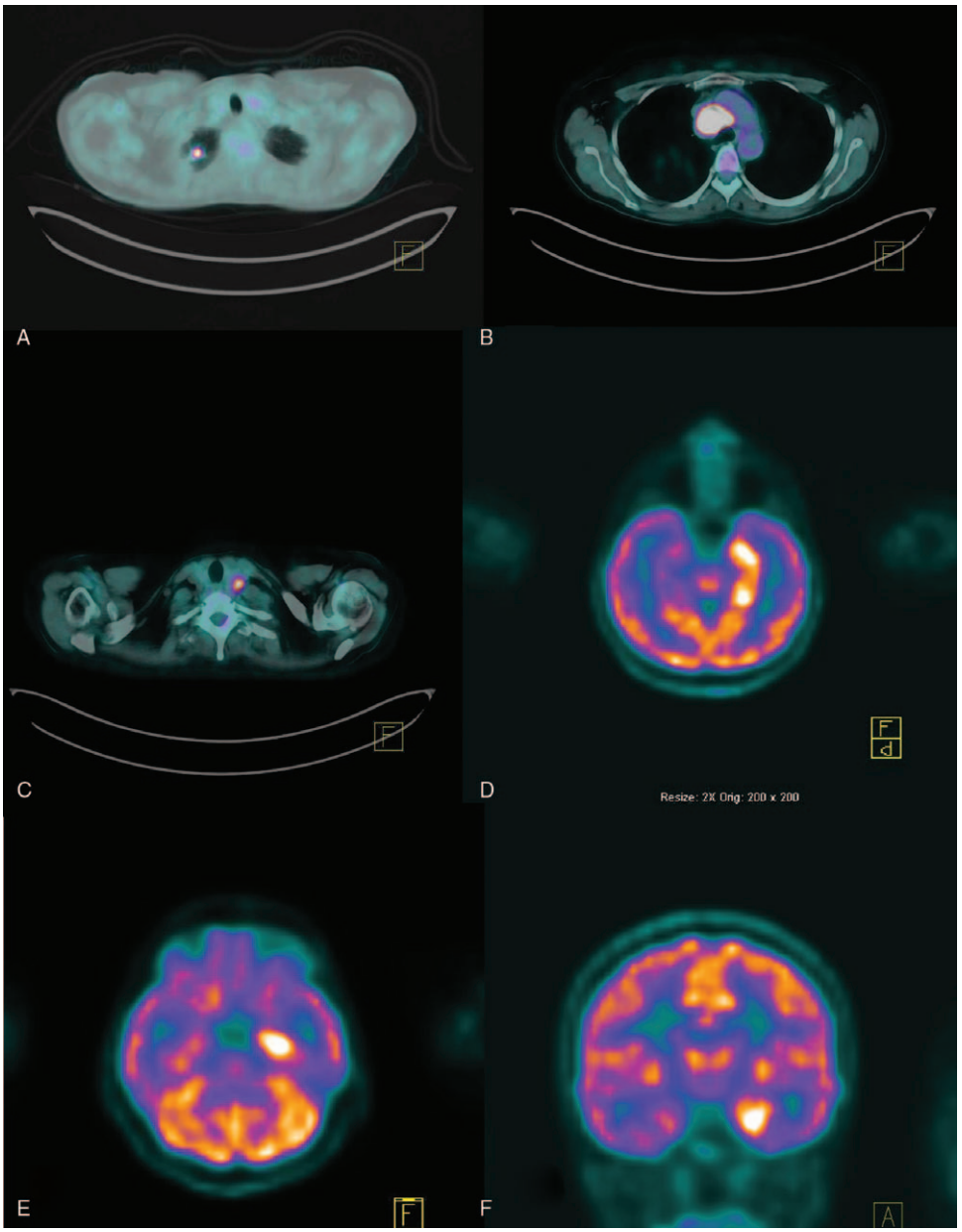

Figure 1. Staging Fluorodeoxyglucose positron emission tomography findings. The initial 18F-FDG PET/CT scan revealed a focal hypermetabolic area at the apex of the right lung with a maximum standardized uptake value (SUV max) of 7.31 (A) and intensely increased activity mass (SUV Max 14.43) in Barety space (B). Focal uptake (SUV Max 5.62) to the left thyroid lobe was noted (C). Functional brain imaging depicted intensely hypermetabolism in the left hippocampus and parahippocampal gyrus and slightly increased activity in antero-superior portion of the right hippocampal on axial (D,E) and coronal planes (F).

From the point of view of the initial clinical picture, our patient presented a subacute onset, with static and dynamic ataxia, and with a progressive trend of neurological symptomatology characterized by difficulty in maintaining the upright position and walking.

Indeed, it was shown that many movement disorders are also immune-mediated. Some of these are paraneoplastic, such as anti-Ma2 hypokinesis and rigidity and anti-Hu ataxia and pseudoathetosis.[11] In our patient, short-term episodic memory deficits arose only after about a month since the diagnosis of the tumor.

Brain MRI showed bilateral abnormalities at the temporal lobes as a sign of possible acute limbic encephalitis with the suspected of an ependymite of the left lateral ventricle. CSF analysis showed signs of inflammation including mild pleocytosis, numerous oligoclonal bands, and intrathecal IgG synthesis. The differential diagnosis was performed with the other disorders that may cause limbic dysfunction. In particular, it was performed with autoimmune systemic disorders such as Sjögren syndrome and Hashimoto encephalopathy because our patient was positive for ANA and ENA SS-A and she had high levels of Thyroperoxidase antibodies and hypothyroidism (in therapy with levothyroxine) for the previous diagnosis of Hashimoto thyroiditis.

Although included in the new criteria for the diagnosis of autoimmune limbic encephalitis, the antibody status is not needed to consider LE as having a definite autoimmune origin,

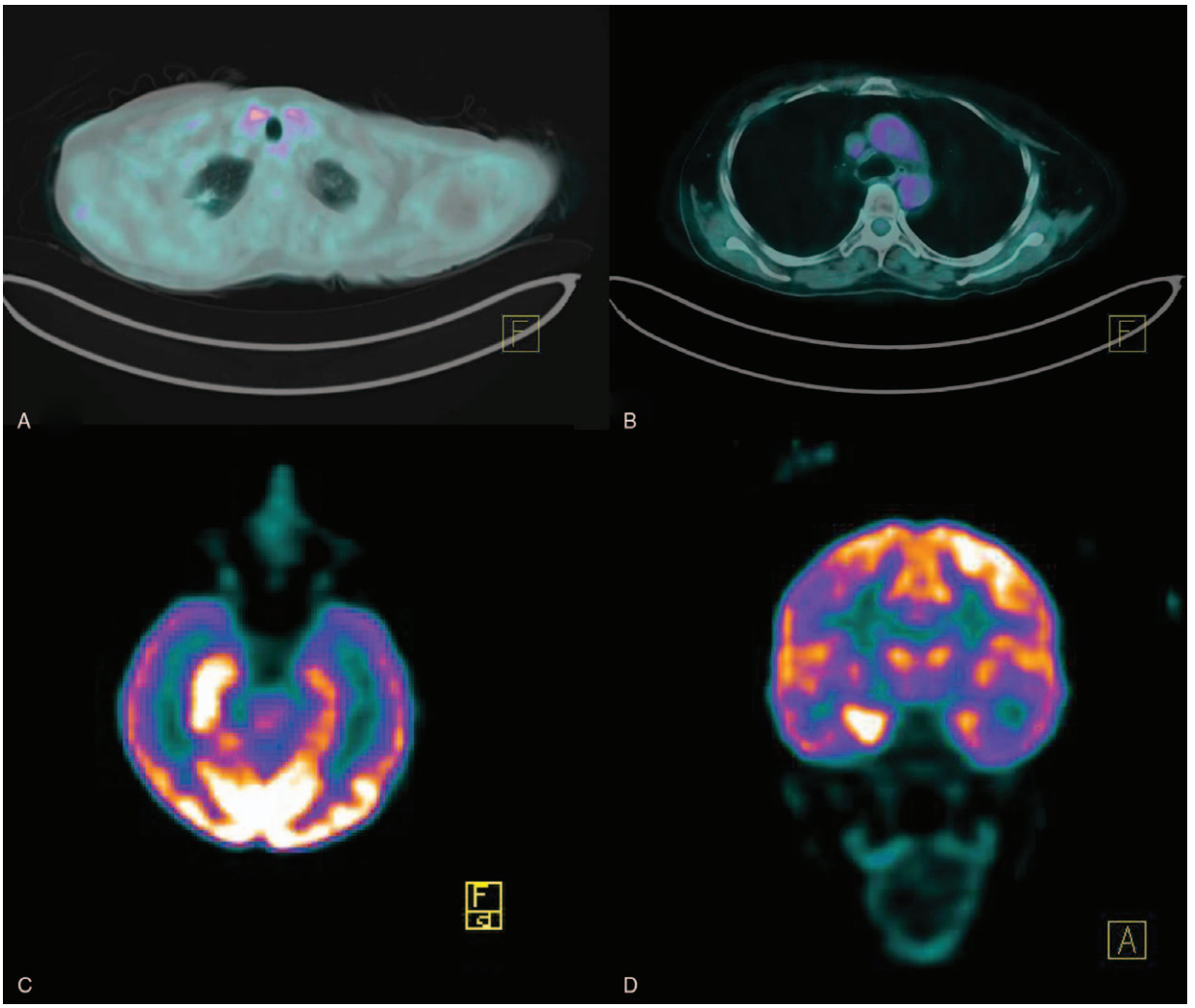

Figure 2. Fluorodeoxyglucose positron emission tomography findings after 3 cycles of chemioterapy. Intense uptake in the right lung disappeared with SUV Max 1.63 vs 7.31 (A). Significant metabolic reduction in Barety space with SUV max 2.24 vs 14.43, on PET/CT scan (B). Functional brain imaging depicted widespread and homogeneous uptake in the right hippocampal and parahippocampal areas and significant metabolic reduction in the left side on axial (C) and coronal planes (D).

measurement of autoantibodies was performed. Numerous studies have shown that their presence is important for classifying LE into subphenotypes according to the location of the target antigens and for determining the prognosis that might differ according to the autoantibody.[2,12–17]

In our patient Anti-Hu e anti-PNMA2 antibodies were positive. It is now known that the onconeuronal antibodies that more frequently occur with LE are Hu and Ma2, and patients who have these antibodies almost always have an underlying cancer.[14,18]

Moreover, the positivity of the NSE was also found. The clinical history, the brain MRI framework, the identification of inflammatory abnormalities in the CSF, and the results of autoantibody testing and cancer biomarker, have increased in our patient the suspicion for paraneoplastic LE.

The presence of an occult pulmonary tumor was confirmed with CT scan and the diagnosis of small cell lung cancer (SCLC) was carried out with EBUS-TBNA of mediastinal lymph node. 18F-FDG PET/CT was performed before the result of the EBUS-TBNA since this method is commonly used in clinical practice for characterizing of the pulmonary nodules and mass lesions.[19]

PET/CT study showed a focal hypermetabolism on the right lung tumor with a Maximum Standardized Uptake Value (SUV Max) higher than the hepatic one. A recent meta-analysis demonstrated that the pre-treatment SUV Max in primary lesions can be an important prognostic factor for overall survival (OS) and event-free survival (EFS) in patients with SCLC.[20] According to the recent National Comprehensive Cancer Network (NCCN) guidelines,[21] the PET scan can increase staging accuracy in patients with SCLC, because SCLC is a highly metabolic disease. If limited-stage disease is suspected, a PET/CT scan can be performed to assess for distant metastases.

Furthermore, for most metastatic sites, the 18F-FDG PET/CT is superior to the CT imaging alone, except for the brain metastasis. In fact, in our patient, the PET/CT scan showed hypermetabolism only on the lymph node in the Barety lodge, while the degree of uptake of the other lymph nodes detected on the CT, was not significant. Although this condition did not affect the staging of our patient's disease, it did play a role in the

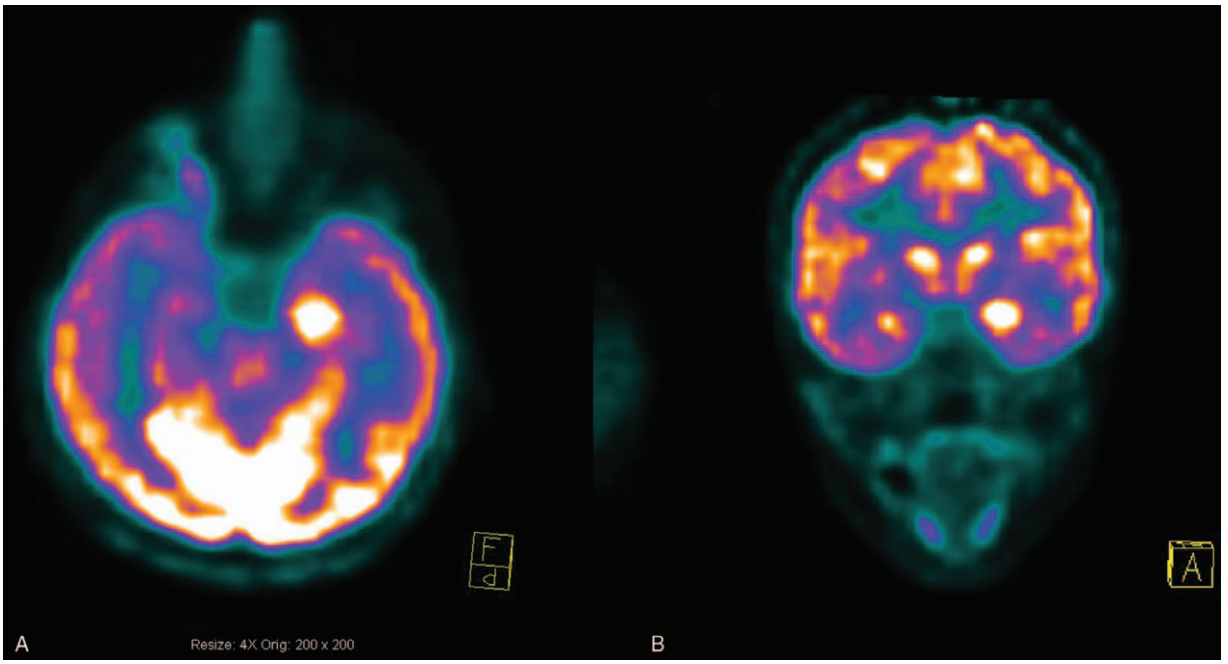

Figure 3. Fluorodeoxyglucose positron emission tomography findings after the end of the chemo-radiotherapeutic treatment. Functional brain imaging revealed less intense hypermetabolism in the right hippocampal and para-hippocampal area and the reappearance of intense uptake in the left hippocampus on axial (A) and coronal planes (B).

planning of the radiotherapy treatment. According to the recent NCCN guidelines,[21] the radiation target volumes can be defined on the PET/CT scan obtained at the time of radiotherapy planning. However, the pre-chemotherapy PET/CT scan should be reviewed to include the originally involved lymph node regions in the treatment fields.

An incidental finding in this case was a focal area of intense glucose uptake at the thyroid gland on the initial 18F-FDG PET/CT. As suggested by Recommendation 15 of the 2015 American Thyroid Association's (ATA's) guidelines,[22] focal 18F-FDG PET/CT uptake in the thyroid is incidentally detected in 1% to 2% of patients and often corresponds to a clinically relevant thyroid nodule on the ultrasound examination. It has been found that the focal glucose uptake increases malignancy risk in an affected nodule and therefore clinical evaluation and FNA of nodules >1 cm is recommended.

Furthermore, in patients with Hashimoto disease or other diffuse thyroidal illnesses, a diffuse thyroid fluorodeoxyglucose PET uptake most often noted. Our patient diagnosed with Hashimoto thyroiditis since 2008, instead presented a left thyroid nodule of 1.7 cm on the ultrasound examination, with a SUV Max of 5.62 at the PET/CT study. A recent meta-analysis confirmed that approximately 1 in 3 (~35%) 18F-FDG PET/CT positive thyroid nodules proved to be cancerous,[23] with higher Mean Maximum Standardized Uptake Value in malignant compared to benign nodules (6.9 vs 4.8, $P < .001$). She was therefore subjected to a FNA of a thyroid nodule and the cytological response was suggestive for the diagnosis of nodular hyperplasia.

Another important finding in the 18F-FDG PET/CT staging, was the metabolic pattern discovered in the brain. It has been demonstrated that brain fluorodeoxyglucose PET is particularly useful in patients without seizures and normal MRI[7] because it can be more sensitive than MRI to show an increase in the FDG uptake in normal-appearing medial temporal lobes.[10] Additionally, 18F-FDG PET of the brain may reveal other areas of hypermetabolism, suggesting additional foci of encephalitis.[7] In this case the functional brain study initially showed an asymmetric hippocampal metabolism with marked and widespread hyperactivity on the left, without any additional hyperactivity sites for the other brain structures. This brain metabolic pattern, in association with the presence of lung and mediastinal lymph node findings at the total-body study, confirmed the diagnostic hypothesis of paraneoplastic LE.

The 18F-FDG PET/CT scan performed after 3 cycles of chemotherapy and at the end of chemo-radiation treatment showed a clear regression of mediastinal lymph node and pulmonary nodule metabolic activity. The evaluation of response therapy assessment is an important aspect of the management of patients with SCLC. Currently, the use of 18F-FDG PET/CT in this setting has not yet been approved. However, some studies assessed metabolic therapeutic responses with FDG PET in SCLC.[24–28] In particular, a recent study[29] compared The European Organization for Research and Treatment of Cancer (EORTC) and Positron Emission Tomography Response Criteria In Solid Tumors (PERCIST) criteria in the evaluation of response assessment in a cohort of SCLC patients and prognostic factors were defined. This study highlighted a perfect concordance between the EORTC and PERCIST criteria. Authors concluded that a complete metabolic response on post-therapeutic FDG PET/CT in patients with SCLC is an important prognostic factor and may help decision making for the therapeutic management.

To evaluate a possible response during the steroid treatment, the PET/CT scans was extended at the brain level. It showed a metabolic behavior characterized by the alternation of intense

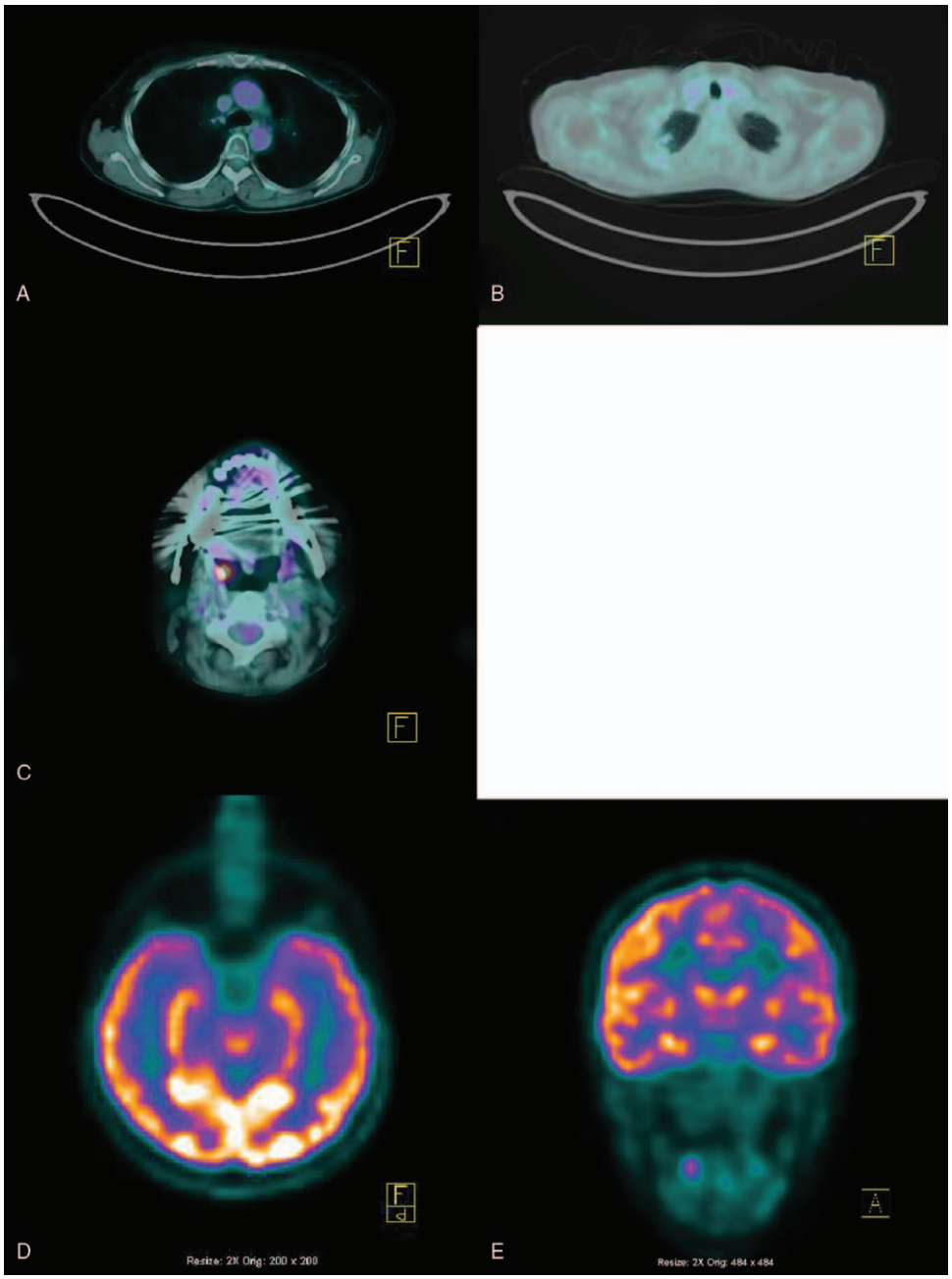

Figure 4. Fluorodeoxyglucose positron emission tomography findings at follow-up. Absence of significant metabolism in the Barety lodge (A) and at the right lung apex on PET/CT scan (B). Focal hypermetabolic area at the right tonsil (C). Functional brain imaging revealed symmetrically decreased 18F-FDG uptake in the medial temporal lobes on axial (D) and coronal planes (E).

hypermetabolism in the bilateral hippocampal areas. This pattern signaled an active inflammatory encephalitic process which correlated with the persistence of clinical symptoms. Only in the last 18F-FDG PET/CT scan a significant metabolic reduction of hippocampal uptake appeared, although it was still above the degree of paraphysiological detection.

In conclusion, we present a patient with PLE combined with SCLC. Our case demonstrates the value of the 18F-FDG PET/CT scan in the assessment of cerebral metabolism in the medial temporal lobe with a metabolic pattern characterized by the migration of hypermetabolism in the bilateral hippocampal areas during the therapeutic treatment. Further investigations would be useful for understanding the pathophysiological mechanisms underlying this process and to evaluate if it is correlated with clinical symptoms and therapeutic responses. Identification of PLE commonly depends on finding cancer. The tumors more frequently involved are SCLC, testicular germ-cell neoplasms, thymoma, Hodgkin lymphoma, or teratoma.[3] Considering that most of these are 18F-FDG avid tumors and that the 18F-FDG PET/CT scan is often added to the diagnostic work-up when screening patients for malignancy, this functional imaging can play a decisive role.

In particular, in this case it also shows that 18F-FDG PET/CT imaging is important and more sensitive than CT alone for the initial staging of SCLC, in the planning of radiotherapy treatment and to evaluate therapeutic response. Finally, in the era of personalized medicine and targeted therapy, this case highlights the importance of the 18F-FDG PET/CT study as an accurate tool to identify PLE and to guide the diagnostic work-up of the underlying tumor.

Author contributions

Conceptualization: Helga Castagnoli, Francesca Capoccetti.
Data curation: Helga Castagnoli.
Formal analysis: Helga Castagnoli.
Investigation: Helga Castagnoli, Carlo Manni, Francesca Marchesani.
Methodology: Francesca Marchesani.
Resources: Francesca Marchesani.
Software: Gloria Rossi, Sara Fattori.
Supervision: Carlo Manni, Gloria Rossi, Francesca Marchesani, Francesca Capoccetti.
Validation: Helga Castagnoli, Gloria Rossi, Sara Fattori, Francesca Capoccetti.
Visualization: Helga Castagnoli, Gloria Rossi.
Writing – original draft: Helga Castagnoli.
Writing – review & editing: Helga Castagnoli, Gloria Rossi, Francesca Marchesani, Francesca Capoccetti.

References

[1] Darnell RB, Posner JB. Paraneoplastic syndromes affecting the nervous system. Semin Oncol 2006;33:270–98.
[2] Ances BM, Vitaliani R, Taylor RA, et al. Treatment-responsive limbic encephalitis identified by neuropil antibodies: MRI and PET correlates. Brain 2005;128:1764–77.
[3] Gultekin SH, Rosenfeld MR, Voltz R, et al. Paraneoplastic limbic encephalitis: neurological symptoms, immunological findings and tumour association in 50 patients. Brain 2000;123:1481–94.
[4] Graus F, Delattre JY, Antoine JC, et al. Recommended diagnostic criteria for paraneoplastic neurological syndromes. J Neurol Neurosurg Psychiatry 2004;75:1135–40.
[5] Kassubek J, Juengling FD, Nitzsche EU, et al. Limbic encephalitis investigated by 18FDG-PET and 3D MRI. J Neuroimaging 2001;11:55–9.
[6] Scheid R, Lincke T, Voltz R, et al. Serial 18F-fluoro-2-deoxy-D-glucose positron emission tomography and magnetic resonance imaging of paraneoplastic limbic encephalitis. Arch Neurol 2004;61:1785–9.
[7] Dalmau J, Bataller L. Clinical and immunological diversity of limbic encephalitis: a model for paraneoplastic neurologic disorders. Hematol Oncol Clin North Am 2006;20:1319–35.
[8] Heine J, Prüss H, Bartsch T, et al. Imaging of autoimmune encephalitis - relevance for clinical practice and hippocampal function. Neuroscience 2015;309:68–83.
[9] Younes-Mhenni S, Janier MF, Cinotti L, et al. FDG-PET improves tumour detection in patients with paraneoplastic neurological syndromes. Brain 2004;127:2331–8.
[10] Graus F, Titulaer MJ, Balu R, et al. A clinical approach to diagnosis of autoimmune encephalitis. Lancet Neurol 2016;15:391–404.
[11] Panzer J, Dalmau J. Movement disorders in paraneoplastic and autoimmune disease. Send to Curr Opin Neurol 2011;24:346–53.
[12] Vincent A, Buckley C, Schott JM, et al. Potassium channel antibody-associated encephalopathy: a potentially immunotherapy-responsive form of limbic encephalitis. Brain 2004;127:701–12.
[13] Dalmau J, Tuzun E, Wu HY, et al. Paraneoplastic anti-N-methyl-D-aspartate receptor encephalitis associated with ovarian teratoma. Ann Neurol 2007;61:25–36.
[14] Dalmau J, Graus F, Villarejo A, et al. Clinical analysis of anti-Ma2-associated encephalitis. Brain 2004;127:1831–44.
[15] Thieben MJ, Lennon VA, Boeve BF, et al. Potentially reversible autoimmune limbic encephalitis with neuronal potassium channel antibody. Neurology 2004;62:1177–82.
[16] Graus F, Keime-Guibert F, Rene R, et al. Anti-Hu-associated paraneoplastic encephalomyelitis: analysis of 200 patients. Brain 2001;124:1138–48.
[17] Tuzun E, Dalmau J. Limbic encephalitis and variants: classification, diagnosis and treatment. Neurologist 2007;13:261–71.
[18] Alamowitch S, Graus F, Uchuya M, et al. Limbic encephalitis and small cell lung cancer. Clinical and immunological features. Brain 1997;120:923–8.
[19] Gould MK, Maclean CC, Kuschner WG, et al. Accuracy of positron emission tomography for diagnosis of pulmonary nodules and mass lesions: a meta-analysis. JAMA 2001;285:914–24.
[20] Zhu D, Wang Y, Wang L, et al. Prognostic value of the maximum standardized uptake value of pre-treatment primary lesions in small-cell lung cancer on 18F-FDG PET/CT: a meta-analysis. Acta Radiol 2018;59:1082–90.
[21] NCCN Clinical Practice Guidelines in Oncology. Small cell lung cancer. Version 2.2018-January 17, 2018.
[22] Haugen BR, Alexander EK, Bible KC, et al. 2015 American Thyroid Association Management Guidelines for adult patients with thyroid nodules and differentiated thyroid cancer: The American Thyroid Association Guidelines Task Force on thyroid nodules and differentiated thyroid cancer. Thyroid 2016;26:1–33.
[23] Soelberg KK, Bonnema SJ, Brix TH, et al. Risk of malignancy in thyroid incidentalomas detected by 18F-fluorodeoxyglucose positron emission tomography: a systematic review. Thyroid 2012;22:918–25.
[24] Azad A, Chionh F, Scott AM, et al. High impact of 18F-FDG-PET on management and prognostic stratification of newly diagnosed small cell lung cancer. Mol Imaging Biol 2010;12:443–51.
[25] Wahl RL, Jacene H, Kasamon Y, et al. From RECIST to PERCIST: evolving considerations for PET response criteria in solid tumors. J Nucl Med 2009;50:122S–50S.
[26] Yamamoto Y, Kameyama R, Murota M, et al. Early assessment of therapeutic response using FDG PET in small cell lung cancer. Mol Imaging Biol 2009;11:467–72.
[27] Mac Manus MP, Hicks RJ, Matthews JP, et al. Positron emission tomography is superior to computed tomography scanning for response-assessment after radical radiotherapy or chemoradiotherapy in patients with non_small-cell lung cancer. J Clin Oncol 2003;21:1285–92.
[28] Fischer BM, Mortensen J, Langer SW, et al. PET/CT imaging in response evaluation of patients with small cell lung cancer. Lung Cancer 2006;54:41–9.
[29] Ziai D, Wagner T, El Badaoui A, et al. Therapy response evaluation with FDG-PET/CT in small cell lung cancer: a prognostic and comparison study of the PERCIST and EORTC criteria. Cancer Imaging 2013;13:73–80.